

25 **ABSTRACT**

26 **Background:** Little is known regarding the long-term adverse effects of COVID-19 on female-
27 specific cancers due to the restricted length of observational time, nor the shared genetic
28 influences underlying these conditions.

29 **Methods:** Leveraging summary statistics from the hitherto largest genome-wide association
30 studies conducted in each trait, we performed a comprehensive genome-wide cross-trait
31 analysis to investigate the shared genetic architecture and the putative genetic associations
32 between COVID-19 with three main female-specific cancers: breast cancer (BC), epithelial
33 ovarian cancer (EOC), and endometrial cancer (EC). Three phenotypes were selected to
34 represent COVID-19 susceptibility (SARS-CoV-2 infection) and severity (COVID-19
35 hospitalization, COVID-19 critical illness).

36 **Results:** For COVID-19 susceptibility, we found no evidence of a genetic correlation with any
37 of the female-specific cancers. For COVID-19 severity, we identified a significant genome-
38 wide genetic correlation with EC for both hospitalization ($r_g=0.19$, $P=0.01$) and critical illness
39 ($r_g=0.29$, $P=3.00\times 10^{-4}$). Mendelian randomization demonstrated no valid association of
40 COVID-19 with any cancer of interest, except for suggestive associations of genetically
41 predicted hospitalization ($OR_{IVW}=1.09$, $95\%CI=1.01-1.18$, $P=0.04$) and critical illness
42 ($OR_{IVW}=1.06$, $95\%CI=1.00-1.11$, $P=0.04$) with EC risk, none withstanding multiple correction.
43 No reverse association was found. Cross-trait meta-analysis identified multiple pleiotropic
44 SNPs between COVID-19 and female-specific cancers, including 20 for BC, 15 for EOC, and
45 5 for EC. Transcriptome-wide association studies revealed shared genes, mostly enriched in the
46 hematologic, cardiovascular, and nervous systems.

47 **Conclusions:** Our genetic analysis highlights an intrinsic link underlying female-specific
48 cancers and COVID-19 - while COVID-19 is not likely to elevate the immediate risk of the
49 examined female-specific cancers, it appears to share mechanistic pathways with these
50 conditions. These findings may provide implications for future therapeutic strategies and public

51 health actions.

52 **Keywords:** COVID-19, SRAS-CoV-2, female-specific cancer, pleiotropic loci, Mendelian

53 randomization, genetic correlation

54 **Introduction**

55 With more than half a billion registered infections and 6.4 million deaths globally, the
56 coronavirus disease 2019 (COVID-19) continues to spread (WHO: <https://covid19.who.int/>).
57 Despite lungs being the organ predominately affected, a multi-system involvement of COVID-
58 19 is well-characterized, with extra-pneumatic manifestations documented in hematologic,
59 cardiovascular, neurological tissues, and others, possibly caused by direct viral virulence or as
60 a result of immunopathological reactions^{1,2}. Moreover, while most COVID-19 patients recover
61 within a couple of weeks after infection, a non-negligible proportion of individuals experience
62 chronic symptoms lasting for months, especially in women^{3,4}. Given the extensive and likely
63 prolonged impairment of COVID-19 on multiple bodily systems, its long-term sequelae have
64 become increasingly recognized and concerning^{3,5}.

65 Strong evidence has been raised reflecting the disparities in COVID-19 pandemic, potentially
66 mediated through unique social determinants of health^{6,7}. Women, especially those with high
67 health burdens are affected disproportionately by COVID-19^{6,8}. For example, individuals with
68 breast cancer (BC) were nearly 3-times more likely to die from COVID-19 than their non-
69 cancer referents (odds ratio, OR = 3.30; 95% confidence interval, 95%CI = 1.96-5.57)⁹. Among
70 women with gynecological cancers, mainly epithelial ovarian cancer (EOC) and endometrial
71 cancer (EC), a significantly increased mortality due to COVID-19 (14.0%)¹⁰ was found
72 compared to general population (5.6%)¹¹. Indeed, several shared signaling pathways, including
73 cytokine, immunosuppression, coagulation disorders, inflammatory reactions, and hormone
74 secretion¹²⁻¹⁵, have been reported. Nevertheless, whether COVID-19 increases the susceptibility
75 to cancer in those without prior malignancies remains unclear due to the hitherto restricted
76 length of observational time. It is concerned that COVID-19 may predispose recovered patients
77 to cancer development based on the growing evidence of SARS-CoV-2 in modulating
78 oncogenic pathways, promoting chronic low-grade inflammation, and causing tissue
79 damage^{12,16}.

80 One way of evaluating the putative causal association underlying two phenotypes is to apply

81 Mendelian randomization (MR)¹⁷, a framework leveraging genetic variants as instruments to
82 overcome the limitation of conventional epidemiological designs, such as restricted
83 observational duration, environmental confounder, and reverse association¹⁸. Using other
84 genetic methods including genetic correlation analysis¹⁹, cross-trait meta-analysis²⁰, and
85 transcriptome-wide association study (TWAS)²¹, shared genetic influences across traits can also
86 be quantified, driving forward epidemiologic associations with novel insights into the
87 underlying biological mechanisms. Here, we apply these methods to perform a comprehensive
88 genome-wide cross-trait analysis¹⁸, with an overarching goal of characterizing the shared
89 genetic architecture and the putative associations underpinning COVID-19 and female-specific
90 cancers (BC, EOC, and EC). Three COVID-19 phenotypes were included, namely SARS-CoV-
91 2 infection, COVID-19 hospitalization, and COVID-19 critical illness. The overview of study
92 design is shown in **Fig 1**.

93

94 **Materials and methods**

95 **GWAS data sets**

96 **Cancer** Three common female malignant tumors, the breast cancer (BC), the epithelial ovarian
97 cancer (EOC), and the endometrial cancer (EC)²², were included in our study. GWAS summary
98 data of BC was obtained from a meta-analysis of the Breast Cancer Association Consortium
99 (BCAC) and 11 other BC genetic studies²³, involving 133,384 cases and 113,789 controls.
100 GWAS summary data of overall invasive EOC was obtained from the Ovarian Cancer
101 Association Consortium (OCAC) meta-analysis²⁴, involving 22,406 cases and 40,941 controls.
102 GWAS summary data of EC was obtained from a meta-analysis of the Endometrial Cancer
103 Association Consortium (ECAC), the Epidemiology of Endometrial Cancer Consortium
104 (E2C2), and the UK Biobank²⁵, involving 12,906 cases and 108,979 controls. All individuals
105 were of European ancestry.

106 **COVID-19** For COVID-19 phenotypes, we used the hitherto largest GWAS summary data of

107 European ancestry conducted by the COVID-19 Host Genetics Initiative, release 7
108 (<https://www.covid19hg.org/>), from which subjects of 23andMe were excluded due to data
109 restrictions²⁶. Three phenotypes were selected and further divided into two categories,
110 representing COVID-19 susceptibility and severity. **SARS-CoV-2 infection**, defined as “cases
111 with reported SARS-CoV-2 infection regardless of symptoms (N = 122,616) vs. population (N
112 = 2,475,240)”, was used to index COVID-19 susceptibility. **COVID-19 hospitalization**,
113 defined as “moderate or severe COVID-19 patients who were hospitalized due to COVID-19
114 symptoms (N = 32,519) vs. population (N = 2,062,805)”, and **COVID-19 critical illness**,
115 defined as “severe COVID-19 patients who needed respiratory support or who died due to the
116 disease (N = 13,769) vs. population (N = 1,072,442)” were used to index COVID-19 severity.
117 Considering a potential sample overlap between GWAS of EC and GWAS of COVID-19
118 phenotypes (both involving UK Biobank subjects), we further performed a sensitivity analysis
119 using trans-ancestry COVID-19 GWAS excluding individuals of UKB. Details on the
120 characteristics of each included dataset are presented in **Supplementary Table 1**.

121 **Statistical analysis**

122 **Genome-wide genetic correlation analysis** To describe the average shared genetic effect
123 between female-specific cancers and COVID-19 phenotypes, we quantified their genome-wide
124 genetic correlation using pairwise linkage-disequilibrium score regression (LDSC)¹⁹. The
125 genetic correlation estimates r_g range from -1 to $+1$, with $+1$ indicating a complete positive
126 correlation and -1 indicating a complete negative correlation. We used pre-computed LD-
127 scores obtained from ~ 1.2 million common SNPs of European ancestry represented in the
128 Hapmap3 reference panel. Bonferroni correction was applied to account for multiple testing.
129 We defined a significant r_g as $P < 5.56 \times 10^{-3}$ ($\alpha = 0.05/9$, number of phenotype pairs)²⁷, and
130 suggestive r_g as $5.56 \times 10^{-3} \leq P < 0.05$.

131 **Bidirectional Mendelian randomization analysis** The average shared genetic effects can be
132 decomposed into vertical pleiotropy and/or horizontal pleiotropy, where vertical pleiotropy (or
133 a putative causal association) refers to genetic variants affecting one trait (outcome) via its

134 effect on an intermediate trait (exposure), and horizontal pleiotropy, often simplified as
135 pleiotropy, refers to genetic variants affecting both traits independently¹⁸. To further explore
136 these alternatives, we first conducted a bidirectional two-sample MR between COVID-19
137 phenotypes and female-specific cancers. As no significant SNP was reported in the original
138 COVID-19 GWAS, we selected independent instrumental variables (IVs) by clumping all
139 variants that reached genome-wide significance ($P < 5 \times 10^{-8}$) according to a strict criterion ($r^2 \leq$
140 0.001 within a 1.0Mb window). For cancers, we collected all previously reported independent
141 index SNPs reaching genome-wide significance ($P < 5 \times 10^{-8}$) from corresponding GWAS. We
142 calculated the F -statistic to evaluate instrument strength, with an F -statistic < 10 indicating a
143 weak instrument²⁸.

144 We applied inverse-variance weighted (IVW) method as our primary approach¹⁷,
145 complemented with MR-Egger²⁹ and weighted median³⁰ to evaluate its robustness. A
146 Bonferroni-corrected significance threshold of $P < 5.56 \times 10^{-3}$ ($\alpha = 0.05/9$, number of phenotype
147 pairs) was applied²⁷, while $5.56 \times 10^{-3} \leq P < 0.05$ was defined as suggestive significance. An MR
148 effect estimate was considered robust if it was statistically significant in IVW and remained
149 directionally consistent across both the MR-Egger and the weighted median approaches.

150 To validate MR model assumptions, we conducted several important sensitivity analyses. First,
151 we excluded palindromic IVs that have the same alleles on forward and reverse strands, and
152 pleiotropic IVs that are associated with potential confounders according to GWAS catalog
153 (<https://www.ebi.ac.uk/gwas/>, accessed on 05/08/2021). Next, we performed a leave-one-out
154 analysis in which we excluded one IV at a time and conducted IVW using the remaining SNPs
155 to identify outlying instruments. Finally, we used MR-Pleiotropy Residual Sum and Outlier
156 (MR-PRESSO) approach to detect and correct for horizontal pleiotropy³¹.

157 **Cross-trait meta-analysis** To identify pleiotropic loci affecting both traits, we further
158 performed a cross-trait meta-analysis using Cross Phenotype Association (CPASSOC)²⁰. We
159 chose S_{Het} , a statistic that is more powerful for heterogenous effects (common when meta-
160 analysing different traits), to combine summary statistics across traits. We used PLINK 1.9

161 “clumping” function to obtain independent loci with parameters: --clump-p1 5e-8 --clump-p2
162 1e-5 --clump-r2 0.2 --clump-kb 500³². Index SNPs, satisfying $P_{CAPSSOC} < 5 \times 10^{-8}$ and $P_{\text{single-trait}} <$
163 1×10^{-3} (both traits), were considered as significant pleiotropic SNPs. An index SNP satisfying
164 the following conditions was considered as a novel shared SNP: (1) did not reach genome-wide
165 significance ($5 \times 10^{-8} < P_{\text{single-trait}} < 1 \times 10^{-3}$) in single-trait GWAS; and (2) was not in LD ($r^2 < 0.05$)
166 with any of the previously reported genome-wide significant SNPs in single-trait GWAS. To
167 further investigate biological insights for the shared variants, we use Ensemble Variant Effect
168 Predictor (VEP) to annotate the linear closest genes of the identified pleiotropic SNPs³³.

169 **Fine-mapping credible set and colocalization analysis** Due to the complex LD patterns
170 among SNPs, index SNPs are not necessarily causal variations³⁴. We conducted a fine-mapping
171 analysis using FM-summary to identify a credible set of variants that were 99% likely to contain
172 causal variants at each of the shared loci. FM-summary is a fine-mapping algorithm in Bayesian
173 framework which maps the primary signal and uses a flat prior with steepest descent
174 approximation³⁵.

175 To assess whether the same variants are responsible for two GWAS signals or are distinct
176 variants close to each other, we conducted a colocalization analysis using Coloc³⁶. Coloc is a
177 tool in Bayesian framework that provides intuitive posterior probabilities of 5 hypotheses (H0-
178 H4). We extracted summary statistics for variants within 500 kb of each shared index SNP and
179 calculated the posterior probability for H4 (PPH4, the probability that both traits are associated
180 through sharing a single causal variant). A locus was considered colocalized if PPH4 was
181 greater than 0.5.

182 **Transcriptome-wide association studies** Many genetic variants implement their function by
183 modulating gene expression in different tissues, thus, considering gene expression and tissue
184 specificity help clarify common biological mechanisms. We performed TWAS to identify genes
185 whose expression is significantly associated with traits using FUSION²¹. We integrated GWAS
186 summary data with expression weights across 48 tissues from GTEx (Genotype-Tissue
187 Expression, version 7), with one tissue-trait pair at a time. Bonferroni-correction was applied

188 for all gene-tissue pairs tested (~230,000 in total) within each trait, and $P_{\text{Bonferroni}} < 0.05$ was
189 defined as significance²⁷. To identify an independent set of gene-tissue pairs, we conducted
190 joint/conditional tests (an extension of TWAS) among regions with multiple identified signals³⁷.
191 Shared gene-tissue pairs were determined through intersection across traits.

192

193 **Results**

194 **Genome-wide genetic correlation** For COVID-19 susceptibility, we found no evidence on a
195 shared genetic basis with any of the female-specific cancers (BC: $r_g = -0.01$, $P = 0.90$; EOC:
196 $r_g = 0.01$, $P = 0.91$; EC: $r_g = 0.09$, $P = 0.23$; **Table 1**). For COVID-19 severity, we identified a
197 suggestive genetic correlation for hospitalization with EC ($r_g = 0.19$, $P = 0.01$), as well as a
198 significant genetic correlation for critical illness with EC ($r_g = 0.29$, $P = 3.00 \times 10^{-4}$). No
199 significant result was found for COVID-19 severity with either BC (hospitalization: $r_g = 0.06$,
200 $P = 0.16$; critical illness: $r_g = 0.05$, $P = 0.28$) or EOC (hospitalization: $r_g = -0.04$, $P = 0.55$;
201 critical illness: $r_g = -0.02$, $P = 0.77$). Interestingly, for EC and COVID-19, both the magnitude
202 and the significance of r_g increased as the disease developed, from infection (0.09) to
203 hospitalization (0.19) to critical illness (0.29).

204 **Bidirectional Mendelian randomization** We continued to conduct a MR to evaluate potential
205 associations of genetically predicted COVID-19 phenotypes on female-specific cancers risk,
206 motivated by the significant shared genetic basis. We identified and selected 16, 38, and 37
207 SNPs as IVs for infection, hospitalization, and critical illness of COVID-19. F -statistics
208 suggested minimal weak instrument bias (**Supplementary Table 2**). **For COVID-19**
209 **susceptibility**, we did not find any association with female-specific cancer (BC: $\text{OR}_{\text{IVW}} = 0.99$,
210 $95\% \text{CI} = 0.86\text{-}1.14$, $P = 0.92$; EOC: $\text{OR}_{\text{IVW}} = 1.19$, $95\% \text{CI} = 0.95\text{-}1.48$, $P = 0.12$; EC: $\text{OR}_{\text{IVW}} =$
211 1.26 , $95\% \text{CI} = 0.97\text{-}1.64$, $P = 0.09$; **Fig 2** and **Supplementary Table 3-4**). **For COVID-19**
212 **severity**, genetically predicted hospitalization ($\text{OR}_{\text{IVW}} = 1.09$, $95\% \text{CI} = 1.01\text{-}1.18$, $P = 0.04$) and
213 critical illness ($\text{OR}_{\text{IVW}} = 1.06$, $95\% \text{CI} = 1.00\text{-}1.11$, $P = 0.04$) were associated with the risk of

214 EC under suggestive significance, none of which withstood multiple correction. The estimates
215 remained directionally consistent using the MR-Egger regression (hospitalization: OR = 1.06,
216 95%CI = 0.91-1.24; critical illness: OR = 1.03, 95%CI = 0.93-1.13) or the weighted median
217 approach (hospitalization: OR = 1.05, 95%CI = 0.95-1.16; critical illness: OR = 1.03, 95%CI =
218 0.97-1.10). No substantial alteration was found after excluding palindromic SNPs or pleiotropic
219 SNPs, and the leave-one-out analysis demonstrated that the pooled estimate was not driven by
220 any outlying variant. MR-PRESSO yielded to similar findings. No association of genetically
221 predicted COVID-19 severity was found for BC (hospitalization: $OR_{IVW} = 1.00$, 95%CI = 0.96-
222 1.05; critical illness: $OR_{IVW} = 1.01$, 95%CI = 0.98-1.04) or EOC (hospitalization: $OR_{IVW} = 1.01$,
223 95%CI = 0.92-1.10; critical illness: $OR_{IVW} = 0.99$, 95%CI = 0.92-1.06).

224 In the reverse-direction MR where female-specific cancers were considered as exposures, we
225 selected 168, 13, and 16 SNPs as IVs to proxy BC, EOC, and EC. *F*-statistics for these IVs
226 suggested strong instruments (**Supplementary Table 5**). None of the three genetically
227 predicted female-specific cancers appeared to affect COVID-19 susceptibility or severity (**Fig**
228 **2 and Supplementary Table 6**).

229 **Cross-trait meta-analysis and pleiotropic loci** With little sign of vertical pleiotropy, we
230 continued to perform cross-trait meta-analysis to reveal horizontal pleiotropic effect of
231 individual variant. A total of 20 independent pleiotropic SNPs were identified as shared by BC
232 with at least one COVID-19 phenotype, including 7 for infection, 7 for hospitalization, and 6
233 for critical illness (**Fig 3 and Supplementary Table 7-10**). These 20 SNPs were mainly located
234 at genomic regions 17q21.31 (harboring *WNT3*, *MAPT*, *CRHR1*, and *PLEKHM1*), 9q34.2
235 (harboring *ABO*, *LCNIP2*, and *REXO4*), and 1q22 (harboring *THBS3*, *GON4L*, and *PMF1*).
236 Notably, SNP rs910416 located at 6q25.1 showed the most significance ($P_{CPASSOC} = 1.90 \times 10^{-29}$),
237 followed by SNP rs17474001 at 9q34.2 ($P_{CPASSOC} = 2.48 \times 10^{-26}$), and SNP rs9411395 at 9q34.2
238 ($P_{CPASSOC} = 4.71 \times 10^{-26}$). We also identified a novel shared locus (index SNP rs1052067,
239 $P_{CPASSOC} = 2.76 \times 10^{-08}$) located at 1q22.

240 A total of 15 independent pleiotropic SNPs were identified as shared by EOC with at least one
241 COVID-19 phenotype, including 5 for infection, 6 for hospitalization, and 4 for critical illness.
242 These 15 SNPs were mainly distributed at 2 loci, 9q34.2 (harboring *ABO*, *SURF4*, and *LCNIP2*)
243 and 17q21.31 (harboring *WNT3*, *MAPT*, *CRHRI*, and *PLEKHMI*). All top-three most
244 significant SNPs were located at 9q34.2, including SNP rs554833 ($P_{\text{CPASSOC}} = 1.28 \times 10^{-88}$), SNP
245 rs657152 ($P_{\text{CPASSOC}} = 6.25 \times 10^{-25}$), and SNP rs56343119 ($P_{\text{CPASSOC}} = 1.28 \times 10^{-22}$).

246 A total of 5 independent pleiotropic SNPs were identified as shared by EC with at least one
247 COVID-19 phenotype, including 2 for infection, 3 for hospitalization, and 2 for critical illness.
248 Three out of the 5 shared SNPs were located at 9q34.2 (harboring *ABO*). Among the rest, SNP
249 rs1123573 was located at 2p16.1 (harboring *BCL11A*), and SNP rs17601876 was located at
250 15q21.2 (harboring *CYP19A1*, *RP11-108K3.1*). Index SNP rs554833 at 9q34.2 showed the most
251 significance ($P_{\text{CPASSOC}} = 3.29 \times 10^{-85}$), followed by SNP rs657152 at 9q34.2 ($P_{\text{CPASSOC}} =$
252 3.77×10^{-26}), and SNP rs17601876 at 15q21.2 ($P_{\text{CPASSOC}} = 3.07 \times 10^{-14}$).

253 **Identification of causal variants and colocalization** For all identified pleiotropic SNPs, we
254 determined a 99% credible set of causal SNPs using FM-summary. A total of 4568 candidate
255 SNPs were identified as the credible set of shared causal SNPs for BC and COVID-19
256 phenotypes. Corresponding figures in EOC and EC were 4893 and 106. Particularly, we
257 identified only one candidate causal SNP in the 99% credible set for BC/infection (rs12216896),
258 BC/hospitalization (rs2887022), and EC/hospitalization (rs1123573). Lists of candidate causal
259 SNPs at each pleiotropic locus were shown in **Supplementary Table 11-13**.

260 We next performed colocalization analysis to determine whether genetic variants driving the
261 association between different traits are the same. We identified several loci to colocalize at the
262 same candidate SNPs ($\text{PPH4} > 0.5$), including 4 shared loci for BC and COVID-19 phenotypes,
263 8 shared loci for EOC and COVID-19 phenotypes, and 3 shared loci for EC and COVID-19
264 phenotypes (**Supplementary Table 14**).

265 **Transcriptome-wide association studies and shared genes** We identified multiple
266 independent gene-tissue pairs shared between female-specific cancers and COVID-19

267 phenotypes (**Table 2**).

268 A total of 11 genes were TWAS-significant for BC with at least one COVID-19 phenotype,
269 including 2 with infection, 7 with hospitalization, and 7 with critical illness, enriched in tissues
270 of adrenal gland, artery, brain, heart, pancreas, skin, stomach and whole blood. Two genes were
271 located at pleiotropic loci identified in cross-trait meta-analysis, including *ABO* (enriched in
272 whole blood and shared by BC with all three COVID-19 phenotypes) and *MSTO2P* (enriched
273 in muscle skeletal and pancreas).

274 A total of 8 genes were TWAS-significant for EOC with at least one COVID-19 phenotype,
275 including one with infection, 7 with hospitalization, and 6 with critical illness, enriched in
276 tissues of artery, adrenal gland, brain, breast mammary, pancreas, and vagina. Among these
277 TWAS significant genes, *ABO* (enriched in artery aorta and shared by EOC with all three
278 COVID-19 phenotypes), *CRHRI-ITI* (enriched in artery aorta and prostate), and *PLEKHMI*
279 (enriched in brain cortex) were located at pleiotropic loci identified in cross-trait meta-analysis.

280 **Sensitivity analysis for sample overlap** A significant genetic correlation between COVID-19
281 severity and EC as well as a suggestive effect of genetically predicted COVID-19 severity on
282 EC risk were identified in the main analysis. Given the sample overlap (both GWASs contained
283 UKB individuals), we additionally conducted a sensitivity analysis applying COVID-19 GWAS
284 excluding UKB subjects. Results of the sensitivity analysis remained consistent with the main
285 analysis, including directionally consistent genome-wide genetic correlation (infection: $r_g =$
286 0.04 , $P = 0.59$; hospitalization: $r_g = 0.14$, $P = 0.03$; critical illness: $r_g = 0.22$, $P = 1.70 \times 10^{-3}$),
287 marginal associations between genetically predicted COVID-19 phenotypes with EC risk
288 (infection: $OR_{IVW} = 1.33$, $95\%CI = 1.06-1.66$; hospitalization: $OR_{IVW} = 1.11$, $95\%CI = 1.03-1.1$;
289 critical illness: $OR_{IVW} = 1.06$, $95\%CI = 1.00-1.12$), as well as 2 replicated pleiotropic SNPs
290 (SNP rs1123573 and SNP rs550057, **Supplementary Tables 15-18**).

291

292 **Discussion**

293 Leveraging the hitherto largest genetic data and novel statistical approaches, the current study
294 performed a comprehensive genome-wide cross-trait analysis to systematically investigate the
295 shared genetic influences underpinning COVID-19 and female-specific malignancies. Our
296 study covered both the susceptibility and severity of COVID-19, as well as the three most
297 common female cancers, BC, EOC, and EC. From a genetic perspective, our work
298 demonstrated biological links underlying these complex traits, highlighting shared mechanisms
299 rather than potential causal associations.

300 COVID-19 presents a broad spectrum of clinical manifestations ranging from asymptomatic
301 infection to death, with the host genetic determinants one of the main influential factors^{2,38}. **For**
302 **COVID-19 susceptibility**, our study suggested no apparent genetic association with any of the
303 examined female-specific cancers. **While for COVID-19 severity**, we found a significant
304 genome-wide genetic correlation for EC with both COVID-19 hospitalization and critical
305 illness, highlighting a non-trivial genetic component that is shared by cancer and a worse
306 symptom of COVID-19. Notably, as the severity of infection develops, the overall COVID-19-
307 EC genetic correlation increases, even with a decreasing sample size of corresponding COVID-
308 19 GWAS. This may be explained by a higher level of plasma cytokines and immune responses
309 in severe COVID-19 patients, both of which are well-established hallmarks for cancer
310 initiation^{39,40}.

311 A shared genetic basis can be the result of vertical pleiotropy and/or horizontal pleiotropy. In
312 our downstream analysis performed to explore these alternatives, we identified no association
313 of genetically predicted **COVID-19 susceptibility** with any cancer of interest, largely in line
314 with the overall null genetic correlation. Two previous studies reported suggestive associations
315 between genetically predicted SARS-CoV-2 infection with EC risk (OR = 1.37, 95%CI = 1.11-
316 1.69; OR = 1.17, 95%CI = 1.01-1.34)^{41,42}. However, these studies applied a limited number of
317 IVs generated from an older version of COVID-19 GWAS (Release 4), which might reduce the
318 precision of MR estimates due to insufficient power. With an eight-times augmented sample
319 size of COVID-19 cases (122,616 vs. 14,134) and a larger number of IVs (16 vs. 3 or 13), our

320 MR did not support for such potential associations. For **COVID-19 severity**, despite suggestive
321 associations identified for genetically predicted hospitalization or critical illness on EC risk,
322 none withstood multiple testing. While these findings were consistent with a previous MR
323 reporting marginal associations (hospitalization: OR = 1.15, 95%CI = 1.00-1.31; critical illness:
324 OR = 1.08, 95%CI = 1.01-1.15)⁴², both the significance and the magnitude of estimates in our
325 study attenuated with a nearly four-times augmented sample size of severe cases
326 (hospitalization: 32,519 vs. 6,404; critical illness: 13,769 vs. 4,336) and a five-times enlarged
327 number of IVs (hospitalization: 38 vs. 7; critical illness: 37 vs. 7). Based on our current findings,
328 a worse symptom of COVID-19 does not seem to represent a risk factor for EC development,
329 while future investigations are warranted to further establish or rule out our findings. By
330 applying a reverse directional MR design, we further confirmed that genetically predicted
331 female-specific cancers appear not to affect either the susceptibility or the severity of COVID-
332 19, concordant with a previous MR study⁴³.

333 Taken together, our MR analysis delivers timely messages that may have important clinical and
334 public health implications. We provide evidence suggesting that COVID-19 is not likely to pose
335 a direct effect on the immediate risk of the examined female-specific cancers, suggesting that
336 extra cancer screening in those recovered from COVID-19 may not confer a substantial public
337 health benefit. In fact, the potential impact of COVID-19 pandemic on routine cancer screening
338 should be given attention, which may lead to an increased burden of cancer mortality⁴⁴.

339 Regarding the inconclusive effect of genetically predicted COVID-19 severity on EC risk, the
340 marginal effect size reflects limited clinical significance. Our study, however, has not ruled out
341 the possibility of subsequent increased risks of other chronic diseases, which, like cancer, is
342 crucial for reducing disease burden and promoting health equity in post-COVID era^{4,5}. To
343 identify other potential long-term sequelae of COVID-19, cancers in other tissues or of other
344 sites, cardiovascular, hematological, neurological diseases, as well as possible long-term
345 chronic inflammation, also require attention.

346 Contrary to the limited genetic evidence observed for vertical pleiotropy, our cross-trait meta-

347 analysis revealed multiple horizontal pleiotropic loci shared between cancers and COVID-19,
348 suggesting that the previously reported phenotypic links could be largely explained by common
349 biological mechanisms. The shared signals identified for both the susceptibility and the severity
350 of COVID-19 further validate the notion that overall genetic correlation may fail to detect
351 pleiotropic effects at individual variant level. Notably, many of our identified cross-trait effects
352 were previously implicated in hematologic systems (*ABO*, *THBS3*)^{38,45}, immune response
353 (*WNT3*, *PLEKHMI*, *BCL11A*, *GON4L*)¹², cell proliferation (*PMF1*, *TTC28*, *KANSL1*), and
354 hormone secretion (*CRHRI*, *ESRI*, *CYP19A1*)^{13,14}, reflecting potential mechanistic pathways
355 linking COVID-19 to tumorigenesis. Via colocalization analysis, multiple genes (*ABO*, *WNT3*,
356 *CUX2*, *SURF4*, *LCNIP2*, *CTD-2612A24.1*, *RP11-430N14.4*) showed strong evidence of a
357 shared causal mechanism (PPH4 > 0.5). Here we highlight two interesting examples, ***ABO*** and
358 ***WNT3***, both are shared by COVID-19 with more than one investigated cancer.

359 ***ABO***, a protein-coding gene involved in blood group systems biosynthesis and coagulation, is
360 a well-known COVID-19 risk gene^{38,46}. In COVID-19 patients, *ABO* contributes to
361 hypercoagulation states and thromboses by affecting plasma glycoproteins⁴⁶⁻⁴⁹, meanwhile,
362 such hypercoagulation states also frequently occurs in many cancer patients^{50,51}. By regulating
363 the circulating levels of several pro-inflammatory and immune adhesion molecules, *ABO* might
364 contribute to both tumorigenesis and COVID-19 development^{52,53}. ***WNT3*** represents a typical
365 immune-related gene, and was identified as a shared gene for COVID-19 severity (rather than
366 susceptibility) with cancer. By activating the WNT/ β -catenin pathway, *WNT3* plays a shaping
367 role in tumor proliferation, migration and invasion, and functions in a variety of pathological
368 processes including inflammation, metabolism, neurological development, and fibrosis
369 processes^{54,55}. Demonstrated by previous studies, upregulation of the canonical WNT/ β -catenin
370 pathway in COVID-19 patients is associated with inflammation and cytokine storm⁵⁶, and such
371 inflammatory immune responses are more likely to occur in patients with severe COVID-19^{39,40}.
372 This may explain why immune-related genes such as *WNT3* were mainly identified to be shared
373 with COVID-19 severity. Our findings suggest critical roles of coagulation and immune

374 responses in both COVID-19 and female-specific cancers regulations, which help pinpoint
375 therapeutic targets for both diseases.

376 Integrating GWAS and GTEx tissue-specific expression data, our TWAS analysis further
377 revealed biological pleiotropy at a gene-tissue pair level. Similar with findings from CPASSOC,
378 we found shared genes between COVID-19 and cancers that are related to hematologic systems
379 (*ABO*), immune function (*MUC1*, *PLEKHM1*), and cell proliferation (*KANSL1-AS1*). The
380 multiple genes identified in blood vessel or heart tissues indicate a biological mechanism
381 through the cardiovascular system, which corroborates well with the established knowledge as
382 both COVID-19 and cancer are associated with a number of cardiovascular complications^{49,57}.

383 In addition, we identified shared regulatory features in the nervous system, especially for
384 COVID-19 severity. In fact, the neuro-invasiveness and neuro-invasion of SARS-CoV-2 have
385 been well-characterized by previous studies, with more than 80% of severe COVID-19 patients
386 showing neurological manifestations during the acute stage of their disease⁵⁸. Through
387 peripheral nerves and/or the hematogenous route, viruses can access the cranial nerves and
388 influence disease manifestation⁵⁸. Moreover, the importance of nervous system in cancer
389 development has also been increasingly recognized⁵⁹. Cancer cells transduce neurotransmitter-
390 mediated intracellular signaling pathways which may lead to their activation, growth, and
391 metastasis⁵⁹. To sum up, these shared biologic pathways for COVID-19 and female-specific
392 cancers implicate therapeutic strategies in clinical practice of the coexisting groups. More
393 studies are needed to fully disclose the complex mechanisms.

394 Several limitations need to be acknowledged. **First**, due to unavailability of data, we conduct
395 our analysis using sex-combined GWAS summary data of COVID-19 which may introduce sex
396 heterogeneity. Future investigations leveraging large-scale sex-specific data may reduce this
397 bias. **Second**, to avoid bias from population stratification, we chose GWAS data restricted to
398 the European ancestry, limiting the generalizability to other ethnic groups. **Third**, the power of
399 our MR analyses could still be limited by sample size, case proportion, and heritability of IVs,
400 leading to the overall negative findings. However, by using data from the hitherto largest GWAS

401 for COVID-19, our overall statistical power was considerably raised compared with previous
402 genetic studies. We had 80% power at an alpha level of 0.05 to detect a 33% increased cancer
403 risk with infection, a 43% increased risk with hospitalization, and a 47% increased risk with
404 critical illness^{60,61}. Larger GWAS data are needed to validate our results in the future. **Finally**,
405 the delineation of COVID-19 susceptibility and severity phenotypes across studies may have
406 been influenced by local social and medical conditions, introducing heterogeneity in the
407 original meta-GWAS that could not be explained in our analysis.

408

409 **Conclusion**

410 Overall, our genetic analysis extends previous findings by highlighting an intrinsic link
411 underlying female-specific cancers and COVID-19. COVID-19 is not likely to elevate the
412 immediate risk of female-specific cancers (BC, EOC, EC), but rather appears to share
413 mechanistic pathways with these conditions. Such common biological mechanisms are
414 specifically substantiated by the pleiotropic loci and shared genes identified in our study,
415 implicating therapeutic strategies for future clinical practice.

416

417 **Competing interests**

418 The authors have declared that no competing interests exist.

419

420 **Acknowledgments**

421 We thank all the patients, staff and investigators who contributed to the COVID-19 Host
422 Genetics Initiative, BCAC consortium, OCAC consortium and ECAC consortium. This study
423 was supported by funds from the National Natural Science Foundation of China (81874283,
424 81673255, 81874282), the National Key R&D Program of China (2020YFC2006505), the
425 Health Commission of Sichuan Province (20PJ093), the Key R&D Program of Sichuan, China

426 (2022YFS0055), the Recruitment Program for Young Professionals of China, the Promotion
427 Plan for Basic Medical Sciences, the Development Plan for Cutting-Edge Disciplines, Sichuan
428 University, and other Projects from West China School of Public Health and West China Fourth
429 Hospital, Sichuan University.

430

431 **Data availability**

432 This study did not generate new datasets or codes. All data used in our study are publicly-
433 available. GWAS summary statistics of the COVID-19 Host Genetics Initiative are accessible
434 at <https://www.covid19hg.org/>. GWAS summary statistics for breast cancer, epithelial ovarian
435 cancer, and endometrial cancer can be downloaded from the GWAS catalog
436 (<https://www.ebi.ac.uk/gwas/>) or from the websites of the consortium
437 (<http://bcac.ccge.medschl.cam.ac.uk/bcacdata/>, <http://ocac.ccge.medschl.cam.ac.uk/>). More
438 details of the approaches as well as the codes are available at <https://github.com/bulik/ldsc>
439 (LDSC), <https://mrcieu.github.io/TwoSampleMR/> (TwoSampleMR),
440 <http://hal.case.edu/~xxz10/zhuweb/> (CPASSOC), [https://github.com/hailianghuang/FM-](https://github.com/hailianghuang/FM-summary)
441 [summary](https://github.com/hailianghuang/FM-summary) (FM-summary), <https://chr1swallace.github.io/coloc/> (Coloc), [https://www.cog-](https://www.cog-genomics.org/plink/1.9/)
442 [genomics.org/plink/1.9/](https://www.cog-genomics.org/plink/1.9/) (PLINK), <https://grch37.ensembl.org/info/docs/tools/vep/index.html>
443 (VEP), <http://gusevlab.org/projects/fusion/> (FUSION).

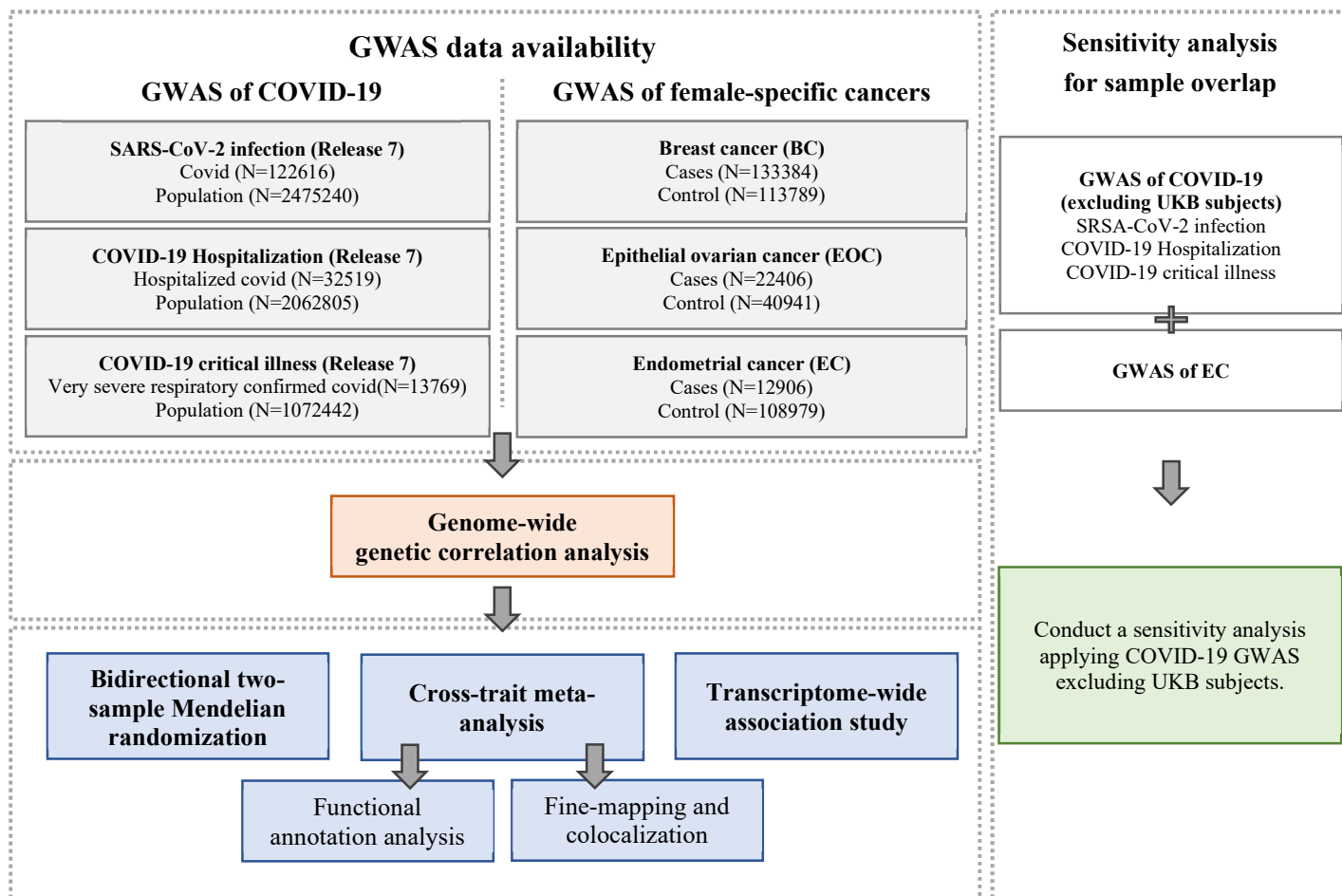
444 **Reference:**

- 445 1 Gupta, A. *et al.* Extrapulmonary manifestations of COVID-19. *Nature medicine* **26**, 1017-1032,
446 doi:10.1038/s41591-020-0968-3 (2020).
- 447 2 Hu, B., Guo, H., Zhou, P. & Shi, Z. L. Characteristics of SARS-CoV-2 and COVID-19. *Nature*
448 *reviews. Microbiology* **19**, 141-154, doi:10.1038/s41579-020-00459-7 (2021).
- 449 3 Brodin, P. Immune determinants of COVID-19 disease presentation and severity. *Nature*
450 *medicine* **27**, 28-33, doi:10.1038/s41591-020-01202-8 (2021).
- 451 4 Sudre, C. H. *et al.* Attributes and predictors of long COVID. *Nature medicine* **27**, 626-631,
452 doi:10.1038/s41591-021-01292-y (2021).
- 453 5 Del Rio, C., Collins, L. F. & Malani, P. Long-term Health Consequences of COVID-19. *Jama*
454 **324**, 1723-1724, doi:10.1001/jama.2020.19719 (2020).
- 455 6 Hawkes, S. *et al.* Recorded but not revealed: exploring the relationship between sex and gender,
456 country income level, and COVID-19. *The Lancet. Global health* **9**, e751-e752,
457 doi:10.1016/s2214-109x(21)00170-4 (2021).
- 458 7 Evans, N. G., Berger, Z. D., Phelan, A. L. & Silverman, R. D. Covid-19, equity, and
459 inclusiveness. *BMJ (Clinical research ed.)* **373**, n1631, doi:10.1136/bmj.n1631 (2021).
- 460 8 Ball, E., Willmott, F., Rivas, C. & Talati, C. COVID-19 in Women's health: Pre-operative
461 gynaecological assessment and shared decision making. *Best practice & research. Clinical*
462 *obstetrics & gynaecology* **73**, 12-21, doi:10.1016/j.bpobgyn.2021.03.001 (2021).
- 463 9 Ruge, M., Zorzi, M. & Guzzinati, S. SARS-CoV-2 infection in the Italian Veneto region:
464 adverse outcomes in patients with cancer. *Nature cancer* **1**, 784-788, doi:10.1038/s43018-020-
465 0104-9 (2020).
- 466 10 Lara, O. D. *et al.* COVID-19 outcomes of patients with gynecologic cancer in New York City:
467 An updated analysis from the initial surge of the pandemic. *Gynecologic oncology* **164**, 304-
468 310, doi:10.1016/j.ygyno.2021.12.004 (2022).
- 469 11 Li, J. *et al.* Epidemiology of COVID-19: A systematic review and meta-analysis of clinical
470 characteristics, risk factors, and outcomes. *Journal of medical virology* **93**, 1449-1458,
471 doi:10.1002/jmv.26424 (2021).
- 472 12 Zong, Z., Wei, Y., Ren, J., Zhang, L. & Zhou, F. The intersection of COVID-19 and cancer:
473 signaling pathways and treatment implications. *Molecular cancer* **20**, 76, doi:10.1186/s12943-
474 021-01363-1 (2021).
- 475 13 Parmar, H. S. *et al.* Cross Talk between COVID-19 and Breast Cancer. *Current cancer drug*
476 *targets* **21**, 575-600, doi:10.2174/1568009621666210216102236 (2021).
- 477 14 Chaudhari, S. *et al.* Comorbidities and inflammation associated with ovarian cancer and its
478 influence on SARS-CoV-2 infection. *Journal of ovarian research* **14**, 39, doi:10.1186/s13048-
479 021-00787-z (2021).
- 480 15 Cai, C., Ahmed, O. A., Shen, H. & Zeng, S. Which cancer type has the highest risk of COVID-
481 19 infection? *The Journal of infection* **81**, 647-679, doi:10.1016/j.jinf.2020.05.028 (2020).
- 482 16 Saini, G. & Aneja, R. Cancer as a prospective sequela of long COVID-19. *BioEssays : news*
483 *and reviews in molecular, cellular and developmental biology* **43**, e2000331,
484 doi:10.1002/bies.202000331 (2021).
- 485 17 Burgess, S., Scott, R. A., Timpson, N. J., Davey Smith, G. & Thompson, S. G. Using published
486 data in Mendelian randomization: a blueprint for efficient identification of causal risk factors.
487 *European journal of epidemiology* **30**, 543-552, doi:10.1007/s10654-015-0011-z (2015).

- 488 18 Zhu, Z., Hasegawa, K., Camargo, C. A., Jr. & Liang, L. Investigating asthma heterogeneity
489 through shared and distinct genetics: Insights from genome-wide cross-trait analysis. *The*
490 *Journal of allergy and clinical immunology* **147**, 796-807, doi:10.1016/j.jaci.2020.07.004
491 (2021).
- 492 19 Bulik-Sullivan, B. *et al.* An atlas of genetic correlations across human diseases and traits. *Nature*
493 *genetics* **47**, 1236-1241, doi:10.1038/ng.3406 (2015).
- 494 20 Zhu, X. *et al.* Meta-analysis of correlated traits via summary statistics from GWASs with an
495 application in hypertension. *American journal of human genetics* **96**, 21-36,
496 doi:10.1016/j.ajhg.2014.11.011 (2015).
- 497 21 Gusev, A. *et al.* Integrative approaches for large-scale transcriptome-wide association studies.
498 *Nature genetics* **48**, 245-252, doi:10.1038/ng.3506 (2016).
- 499 22 Sung, H. *et al.* Global Cancer Statistics 2020: GLOBOCAN Estimates of Incidence and
500 Mortality Worldwide for 36 Cancers in 185 Countries. *CA: a cancer journal for clinicians* **71**,
501 209-249, doi:10.3322/caac.21660 (2021).
- 502 23 Zhang, H. *et al.* Genome-wide association study identifies 32 novel breast cancer susceptibility
503 loci from overall and subtype-specific analyses. *Nature genetics* **52**, 572-581,
504 doi:10.1038/s41588-020-0609-2 (2020).
- 505 24 Phelan, C. M. *et al.* Identification of 12 new susceptibility loci for different histotypes of
506 epithelial ovarian cancer. *Nature genetics* **49**, 680-691, doi:10.1038/ng.3826 (2017).
- 507 25 O'Mara, T. A. *et al.* Identification of nine new susceptibility loci for endometrial cancer. *Nature*
508 *communications* **9**, 3166, doi:10.1038/s41467-018-05427-7 (2018).
- 509 26 The COVID-19 Host Genetics Initiative, a global initiative to elucidate the role of host genetic
510 factors in susceptibility and severity of the SARS-CoV-2 virus pandemic. *European journal of*
511 *human genetics : EJHG* **28**, 715-718, doi:10.1038/s41431-020-0636-6 (2020).
- 512 27 Bland, J. M. & Altman, D. G. Multiple significance tests: the Bonferroni method. *BMJ (Clinical*
513 *research ed.)* **310**, 170, doi:10.1136/bmj.310.6973.170 (1995).
- 514 28 Burgess, S. & Thompson, S. G. Avoiding bias from weak instruments in Mendelian
515 randomization studies. *International journal of epidemiology* **40**, 755-764,
516 doi:10.1093/ije/dyr036 (2011).
- 517 29 Bowden, J., Davey Smith, G. & Burgess, S. Mendelian randomization with invalid instruments:
518 effect estimation and bias detection through Egger regression. *International journal of*
519 *epidemiology* **44**, 512-525, doi:10.1093/ije/dyv080 (2015).
- 520 30 Bowden, J., Davey Smith, G., Haycock, P. C. & Burgess, S. Consistent Estimation in Mendelian
521 Randomization with Some Invalid Instruments Using a Weighted Median Estimator. *Genetic*
522 *epidemiology* **40**, 304-314, doi:10.1002/gepi.21965 (2016).
- 523 31 Verbanck, M., Chen, C. Y., Neale, B. & Do, R. Detection of widespread horizontal pleiotropy
524 in causal relationships inferred from Mendelian randomization between complex traits and
525 diseases. *Nature genetics* **50**, 693-698, doi:10.1038/s41588-018-0099-7 (2018).
- 526 32 Purcell, S. *et al.* PLINK: a tool set for whole-genome association and population-based linkage
527 analyses. *American journal of human genetics* **81**, 559-575, doi:10.1086/519795 (2007).
- 528 33 Howe, K. L. *et al.* Ensembl 2021. *Nucleic acids research* **49**, D884-d891,
529 doi:10.1093/nar/gkaa942 (2021).
- 530 34 Schaid, D. J., Chen, W. & Larson, N. B. From genome-wide associations to candidate causal
531 variants by statistical fine-mapping. *Nature reviews. Genetics* **19**, 491-504, doi:10.1038/s41576-

- 532 018-0016-z (2018).
- 533 35 Farh, K. K. *et al.* Genetic and epigenetic fine mapping of causal autoimmune disease variants.
534 *Nature* **518**, 337-343, doi:10.1038/nature13835 (2015).
- 535 36 Giambartolomei, C. *et al.* Bayesian test for colocalisation between pairs of genetic association
536 studies using summary statistics. *PLoS genetics* **10**, e1004383,
537 doi:10.1371/journal.pgen.1004383 (2014).
- 538 37 Gusev, A. *et al.* Transcriptome-wide association study of schizophrenia and chromatin activity
539 yields mechanistic disease insights. *Nature genetics* **50**, 538-548, doi:10.1038/s41588-018-
540 0092-1 (2018).
- 541 38 Mapping the human genetic architecture of COVID-19. *Nature* **600**, 472-477,
542 doi:10.1038/s41586-021-03767-x (2021).
- 543 39 Yang, X. *et al.* Clinical course and outcomes of critically ill patients with SARS-CoV-2
544 pneumonia in Wuhan, China: a single-centered, retrospective, observational study. *The Lancet.*
545 *Respiratory medicine* **8**, 475-481, doi:10.1016/s2213-2600(20)30079-5 (2020).
- 546 40 Huang, C. *et al.* Clinical features of patients infected with 2019 novel coronavirus in Wuhan,
547 China. *Lancet (London, England)* **395**, 497-506, doi:10.1016/s0140-6736(20)30183-5 (2020).
- 548 41 Gao, R. *et al.* Genetic variation associated with COVID-19 is also associated with endometrial
549 cancer. *The Journal of infection* **84**, e85-e86, doi:10.1016/j.jinf.2022.01.026 (2022).
- 550 42 Wu, X. *et al.* Novel evidence revealed genetic association between COVID-19 infection,
551 severity and endometrial cancer. *The Journal of infection* **85**, e1-e3,
552 doi:10.1016/j.jinf.2022.05.005 (2022).
- 553 43 Li, Z., Wei, Y., Zhu, G., Wang, M. & Zhang, L. Cancers and COVID-19 Risk: A Mendelian
554 Randomization Study. *Cancers* **14**, doi:10.3390/cancers14092086 (2022).
- 555 44 Janda, M., Paul, C. & Horsham, C. Changes in cancer preventive behaviours, screening and
556 diagnosis during COVID-19. *Psycho-oncology* **30**, 271-273, doi:10.1002/pon.5575 (2021).
- 557 45 Zhang, C. *et al.* The Integrative Analysis of Thrombospondin Family Genes in Pan-Cancer
558 Reveals that THBS2 Facilitates Gastrointestinal Cancer Metastasis. *Journal of oncology* **2021**,
559 4405491, doi:10.1155/2021/4405491 (2021).
- 560 46 Hernández Cordero, A. I. *et al.* Multi-omics highlights ABO plasma protein as a causal risk
561 factor for COVID-19. *Human genetics* **140**, 969-979, doi:10.1007/s00439-021-02264-5 (2021).
- 562 47 Matsui, T., Titani, K. & Mizuochi, T. Structures of the asparagine-linked oligosaccharide chains
563 of human von Willebrand factor. Occurrence of blood group A, B, and H(O) structures. *The*
564 *Journal of biological chemistry* **267**, 8723-8731 (1992).
- 565 48 Teuwen, L. A., Geldhof, V., Pasut, A. & Carmeliet, P. COVID-19: the vasculature unleashed.
566 *Nature reviews. Immunology* **20**, 389-391, doi:10.1038/s41577-020-0343-0 (2020).
- 567 49 Franchini, M., Favaloro, E. J., Targher, G. & Lippi, G. ABO blood group, hypercoagulability,
568 and cardiovascular and cancer risk. *Critical reviews in clinical laboratory sciences* **49**, 137-149,
569 doi:10.3109/10408363.2012.708647 (2012).
- 570 50 Falanga, A., Marchetti, M. & Vignoli, A. Coagulation and cancer: biological and clinical aspects.
571 *Journal of thrombosis and haemostasis : JTH* **11**, 223-233, doi:10.1111/jth.12075 (2013).
- 572 51 Rodrigues, C. A., Ferrarotto, R., Kalil Filho, R., Novis, Y. A. & Hoff, P. M. Venous
573 thromboembolism and cancer: a systematic review. *Journal of thrombosis and thrombolysis* **30**,
574 67-78, doi:10.1007/s11239-010-0441-0 (2010).
- 575 52 Barbalic, M. *et al.* Large-scale genomic studies reveal central role of ABO in sP-selectin and

576 sICAM-1 levels. *Human molecular genetics* **19**, 1863-1872, doi:10.1093/hmg/ddq061 (2010).
577 53 Paterson, A. D. *et al.* Genome-wide association identifies the ABO blood group as a major locus
578 associated with serum levels of soluble E-selectin. *Arteriosclerosis, thrombosis, and vascular*
579 *biology* **29**, 1958-1967, doi:10.1161/atvbaha.109.192971 (2009).
580 54 Grainger, S. & Willert, K. Mechanisms of Wnt signaling and control. *Wiley interdisciplinary*
581 *reviews. Systems biology and medicine*, e1422, doi:10.1002/wsbm.1422 (2018).
582 55 Liu, J. *et al.* Wnt/ β -catenin signalling: function, biological mechanisms, and therapeutic
583 opportunities. *Signal transduction and targeted therapy* **7**, 3, doi:10.1038/s41392-021-00762-6
584 (2022).
585 56 Vallée, A., Lecarpentier, Y. & Vallée, J. N. Interplay of Opposing Effects of the WNT/ β -Catenin
586 Pathway and PPAR γ and Implications for SARS-CoV2 Treatment. *Frontiers in immunology* **12**,
587 666693, doi:10.3389/fimmu.2021.666693 (2021).
588 57 Roh, J. D. *et al.* Plasma Proteomics of COVID-19-Associated Cardiovascular Complications:
589 Implications for Pathophysiology and Therapeutics. *JACC. Basic to translational science* **7**,
590 425-441, doi:10.1016/j.jacbts.2022.01.013 (2022).
591 58 Bauer, L. *et al.* The neuroinvasiveness, neurotropism, and neurovirulence of SARS-CoV-2.
592 *Trends in neurosciences* **45**, 358-368, doi:10.1016/j.tins.2022.02.006 (2022).
593 59 Kuol, N., Stojanovska, L., Apostolopoulos, V. & Nurgali, K. Role of the nervous system in
594 cancer metastasis. *Journal of experimental & clinical cancer research : CR* **37**, 5,
595 doi:10.1186/s13046-018-0674-x (2018).
596 60 Shim, H. *et al.* A multivariate genome-wide association analysis of 10 LDL subfractions, and
597 their response to statin treatment, in 1868 Caucasians. *PloS one* **10**, e0120758,
598 doi:10.1371/journal.pone.0120758 (2015).
599 61 Brion, M. J., Shakhbazov, K. & Visscher, P. M. Calculating statistical power in Mendelian
600 randomization studies. *International journal of epidemiology* **42**, 1497-1501,
601 doi:10.1093/ije/dyt179 (2013).
602



603

604 **Fig 1. Overall study design of genome-wide cross-trait analysis.** GWAS summary statistics
 605 for each trait of interest were retrieved from publicly available GWAS(s). GWAS: genome-
 606 wide association study; UKB: UK Biobank.

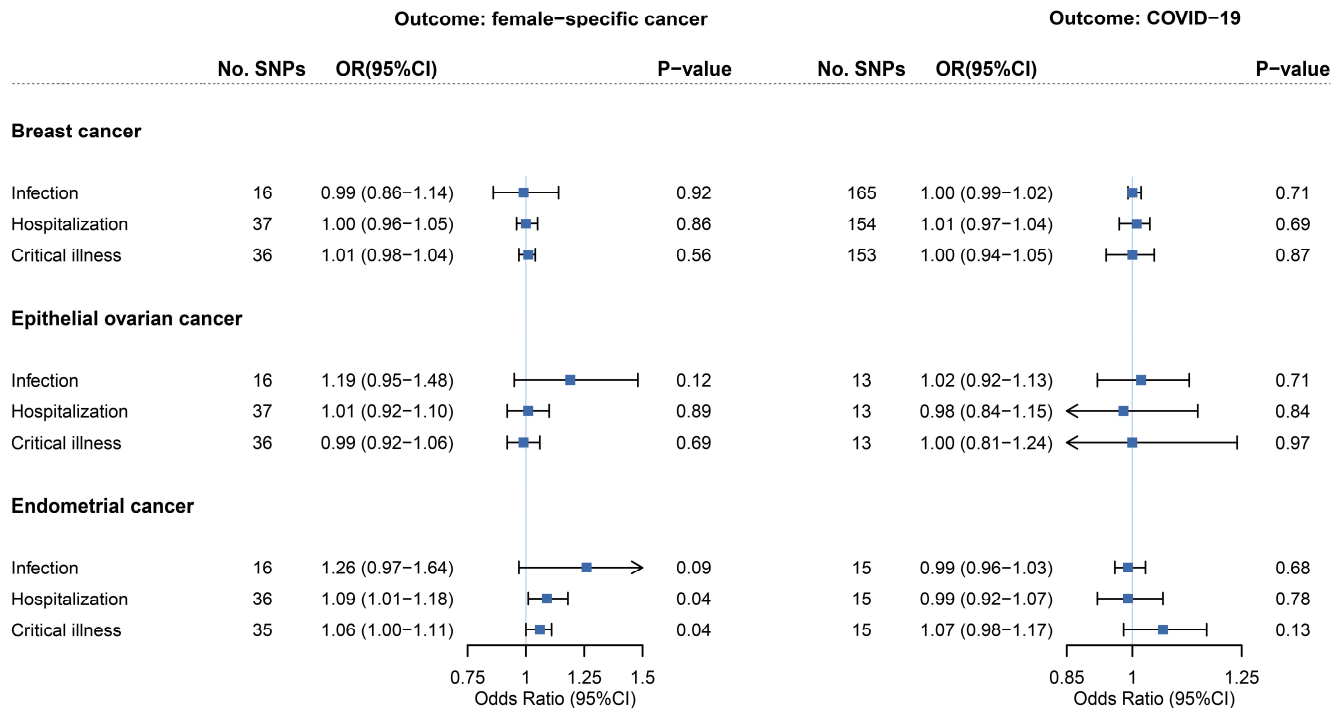
607

Table 1. Genetic correlation between female-specific cancers and COVID-19 phenotypes.

Cancer	COVID-19 phenotype	r_g	95%CI	P-value
BC	Infection	-0.01	(-0.09,0.08)	0.90
	Hospitalization	0.06	(-0.02,0.14)	0.16
	Critical illness	0.05	(-0.04,0.13)	0.28
EOC	Infection	0.01	(-0.16,0.18)	0.91
	Hospitalization	-0.04	(-0.19,0.10)	0.55
	Critical illness	-0.02	(-0.17,0.13)	0.77
EC	Infection	0.09	(-0.06,0.24)	0.23
	Hospitalization	0.19	(0.04,0.34)	0.01
	Critical illness	0.29	(0.14,0.45)	3.00×10^{-4}*

Bold-face: $P < 0.05$; * $P < 5.56 \times 10^{-3}$.

r_g : genetic correlation; CI: confidence interval; Infection: reported SARS-CoV-2 infection vs. population; Hospitalization: COVID-19 hospitalization patients vs. population; Critical illness: very severe respiratory confirmed COVID-19 patients vs. population; BC: breast cancer; EOC: overall invasive epithelial ovarian cancer; EC: endometrial cancer



609

610 **Fig 2. Bidirectional Mendelian randomization associations between COVID-19**

611 **phenotypes and female-specific cancers.** On the left are the MR effect estimates of

612 genetically predicted COVID-19 phenotypes on each female-specific cancer by the inverse-

613 variance weighted approach. On the right are the MR effect estimates of genetically predicted

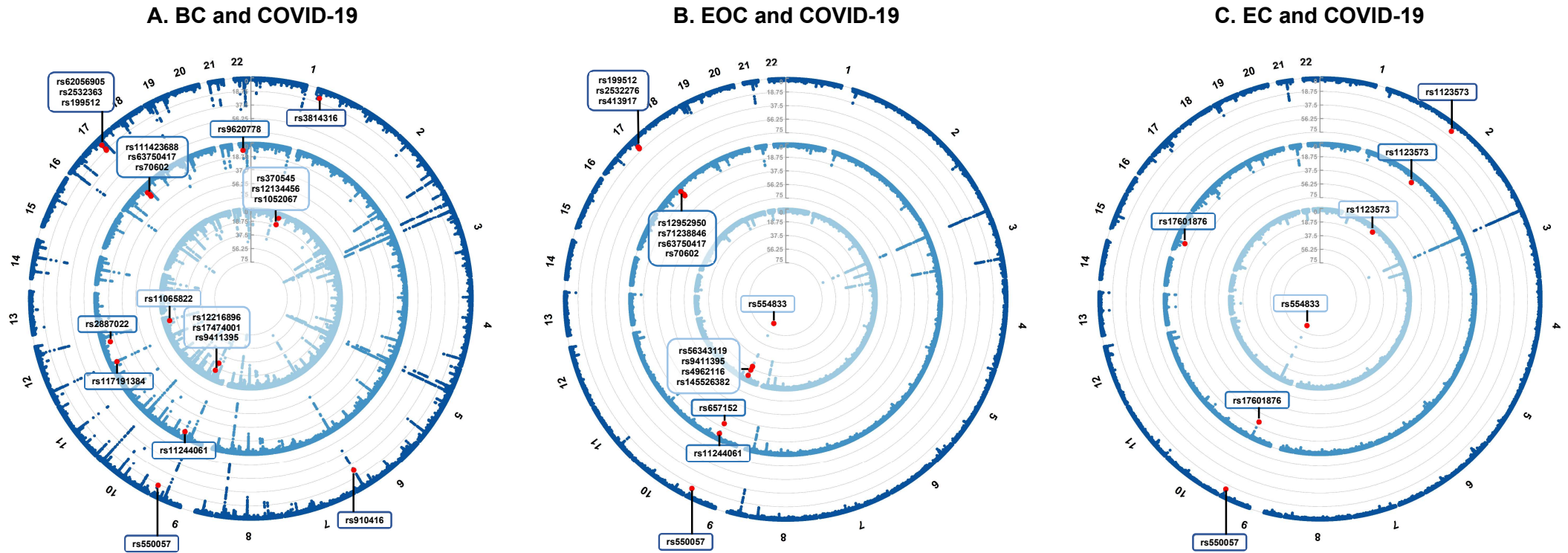
614 female-specific cancer on COVID-19 phenotypes by the inverse-variance weighted approach.

615 Boxes represent the point estimates of MR effects, and error bars represent 95% confidence

616 intervals.

617

618



619
620 **Fig 3. Pleiotropic loci between female-specific cancers and COVID-19 phenotypes identified from cross-trait meta-analysis.** (A) Pleiotropic loci identified for breast
621 cancer and COVID-19 phenotypes; (B) pleiotropic loci identified for epithelial ovarian cancer and COVID-19 phenotypes; (C) pleiotropic loci identified for endometrial cancer
622 and COVID-19 phenotypes. In each circular Manhattan plot, the circle from center to periphery shows the cross-trait meta-analysis results between each female-specific cancer
623 and the three COVID-19 phenotypes (light blue: SRAS-CoV-2 infection, blue: COVID-19 hospitalization, dark blue: COVID-19 critical illness). The outermost numbers
624 represent chromosomes 1-22. The red dots represent significant pleiotropic SNPs in cross-trait meta-analysis ($P_{\text{CPASSOC}} < 5 \times 10^{-8}$ and $P_{\text{single-trait}} < 1 \times 10^{-3}$ in both traits).

Table 2. TWAS-identified shared gene-tissue pairs between COVID-19 and female-specific cancers after conditional and joint analysis.

Gene	Tissue Type	CHR	No. SNPs	Female-specific cancer					COVID-19		
				Type	BEST. GWAS.ID	Z	$P_{\text{Bonferroni}}$	Subtype	BEST. GWAS.ID	Z	$P_{\text{Bonferroni}}$
Breast cancer and COVID-19											
GBAP1	Adrenal Gland	1	328	BC	rs4971059	-6.73	3.89×10^{-6}	Infection	rs11264339	7.05	4.06×10^{-7}
GBAP1	Artery Aorta	1	328	BC	rs4971059	-6.49	1.96×10^{-5}	Infection	rs11264339	7.24	1.04×10^{-7}
GBAP1	Artery Coronary	1	328	BC	rs4971059	-5.68	3.10×10^{-3}	Infection	rs11264339	7.09	3.02×10^{-7}
GBAP1	Artery Tibial	1	328	BC	rs4971059	-6.30	7.05×10^{-5}	Infection	rs11264339	6.97	7.24×10^{-7}
GBAP1	Cells Transformed fibroblasts	1	328	BC	rs4971059	-6.44	2.72×10^{-5}	Infection	rs11264339	7.13	2.34×10^{-7}
GBAP1	Esophagus Muscularis	1	328	BC	rs4971059	-6.71	4.68×10^{-6}	Infection	rs11264339	6.80	2.39×10^{-6}
GBAP1	Heart Atrial Appendage	1	328	BC	rs4971059	-5.68	3.10×10^{-3}	Infection	rs11264339	7.09	3.02×10^{-7}
GBAP1	Skin Not Sun Exposed Suprapubic	1	328	BC	rs4971059	-6.84	1.79×10^{-6}	Infection	rs11264339	7.00	5.92×10^{-7}
GBAP1	Skin Sun Exposed Lower leg	1	328	BC	rs4971059	-6.62	8.19×10^{-6}	Infection	rs11264339	7.05	4.04×10^{-7}
ABO	Whole Blood	9	595	BC	rs495828	-5.34	2.15×10^{-2}	Infection	rs612169	-10.05	2.24×10^{-18}
KANSL1-AS1	Artery Coronary	17	29	BC	rs17763086	-6.03	3.93×10^{-4}	Hospitalization	rs8072451	-7.57	8.91×10^{-9}
KANSL1-AS1	Brain Anterior cingulate cortex BA24	17	29	BC	rs17763086	-6.03	3.93×10^{-4}	Hospitalization	rs8072451	-7.57	8.91×10^{-9}
RP11-259G18.1	Brain Cortex	17	66	BC	rs17763086	-6.03	3.93×10^{-4}	Hospitalization	rs8072451	-7.57	8.91×10^{-9}
CRHR1-IT1	Stomach	17	93	BC	rs17763086	-6.03	3.93×10^{-4}	Hospitalization	rs8072451	-7.57	8.91×10^{-9}
RPS26P8	Pituitary	17	106	BC	rs17763086	-6.03	3.93×10^{-4}	Hospitalization	rs8072451	-7.57	8.91×10^{-9}
RP11-707O23.5	Artery Tibial	17	111	BC	rs17763086	-6.15	1.77×10^{-4}	Hospitalization	rs8072451	-7.87	7.98×10^{-10}
RP11-707O23.5	Brain Hypothalamus	17	111	BC	rs17763086	-6.03	3.72×10^{-4}	Hospitalization	rs8072451	-7.58	7.84×10^{-9}
LRRC37A4P	Adrenal Gland	17	138	BC	rs17763086	6.03	3.93×10^{-4}	Hospitalization	rs8072451	7.57	8.91×10^{-9}
LRRC37A4P	Heart Left Ventricle	17	138	BC	rs17763086	6.07	3.05×10^{-4}	Hospitalization	rs8072451	7.65	4.79×10^{-9}
ABO	Whole Blood	9	595	BC	rs495828	-5.34	2.15×10^{-2}	Hospitalization	rs657152	-5.70	2.80×10^{-3}
RP11-707O23.5	Artery Tibial	17	111	BC	rs17763086	-6.15	1.77×10^{-4}	Critical illness	rs16940665	-7.59	7.13×10^{-9}
RP11-707O23.5	Brain Hypothalamus	17	111	BC	rs17763086	-6.03	3.72×10^{-4}	Critical illness	rs16940665	-7.40	3.10×10^{-8}
LRRC37A4P	Brain Nucleus accumbens basal ganglia	17	138	BC	rs17763086	6.03	3.82×10^{-4}	Critical illness	rs16940665	7.45	2.13×10^{-8}
MSTO2P	Muscle Skeletal	1	236	BC	rs11264372	-6.45	2.65×10^{-5}	Critical illness	rs11803917	-5.70	2.73×10^{-3}
MSTO2P	Pancreas	1	236	BC	rs11264372	-6.28	7.94×10^{-5}	Critical illness	rs11803917	-5.43	1.32×10^{-2}
HCN3	Brain Nucleus accumbens basal ganglia	1	298	BC	rs4971059	-7.75	2.13×10^{-9}	Critical illness	rs35154152	-5.38	1.73×10^{-2}
GBAP1	Brain Cerebellum	1	328	BC	rs4971059	-7.01	5.75×10^{-7}	Critical illness	rs35154152	-5.44	1.23×10^{-2}

MUC1	Pancreas	1	339	BC	rs4971059	6.47	2.24×10^{-5}	Critical illness	rs35154152	5.25	3.59×10^{-2}
ABO	Whole Blood	9	595	BC	rs495828	-5.34	2.15×10^{-2}	Critical illness	rs657152	-5.57	5.98×10^{-3}
Epithelial ovarian cancer and COVID-19											
ABO	Artery Aorta	9	595	EOC	rs495828	5.60	4.92×10^{-3}	Infection	rs612169	17.33	6.75×10^{-62}
KANSL1-AS1	Brain Anterior cingulate cortex BA24	17	29	EOC	rs4566211	7.08	3.35×10^{-7}	Hospitalization	rs8072451	-7.57	8.91×10^{-9}
KANSL1-AS1	Vagina	17	29	EOC	rs4566211	7.10	2.87×10^{-7}	Hospitalization	rs8072451	-7.54	1.05×10^{-8}
RP11-259G18.2	Small Intestine Terminal Ileum	17	59	EOC	rs4566211	7.16	1.82×10^{-7}	Hospitalization	rs8072451	-7.58	7.80×10^{-9}
CRHR1-IT1	Artery Aorta	17	93	EOC	rs17631676	7.11	2.66×10^{-7}	Hospitalization	rs8072451	-7.55	9.99×10^{-9}
CRHR1-IT1	Prostate	17	93	EOC	rs17631676	7.10	2.87×10^{-7}	Hospitalization	rs8072451	-7.54	1.05×10^{-8}
RPS26P8	Breast Mammary Tissue	17	106	EOC	rs17631676	7.08	3.35×10^{-7}	Hospitalization	rs8072451	-7.57	8.91×10^{-9}
RPS26P8	Pituitary	17	106	EOC	rs17631676	7.08	3.35×10^{-7}	Hospitalization	rs8072451	-7.57	8.91×10^{-9}
LRRC37A4P	Adrenal Gland	17	138	EOC	rs17631676	-7.08	3.35×10^{-7}	Hospitalization	rs8072451	7.57	8.91×10^{-9}
PLEKHM1	Brain Cortex	17	162	EOC	rs17631676	7.25	9.99×10^{-8}	Hospitalization	rs8072451	-5.19	5.00×10^{-2}
ABO	Artery Aorta	9	595	EOC	rs495828	5.60	4.92×10^{-3}	Hospitalization	rs657152	8.79	3.49×10^{-13}
KANSL1-AS1	Pancreas	17	29	EOC	rs4566211	7.12	2.61×10^{-7}	Critical illness	rs16940665	-7.42	2.83×10^{-8}
KANSL1-AS1	Vagina	17	29	EOC	rs4566211	7.10	2.87×10^{-7}	Critical illness	rs16940665	-7.45	2.18×10^{-8}
RP11-259G18.2	Small Intestine Terminal Ileum	17	59	EOC	rs4566211	7.16	1.82×10^{-7}	Critical illness	rs16940665	-7.52	1.29×10^{-8}
RP11-259G18.1	Brain Hippocampus	17	65	EOC	rs4566211	7.11	2.66×10^{-7}	Critical illness	rs16940665	-7.46	1.94×10^{-8}
CRHR1-IT1	Artery Aorta	17	93	EOC	rs17631676	7.11	2.66×10^{-7}	Critical illness	rs16940665	-7.46	1.94×10^{-8}
LRRC37A4P	Brain Amygdala	17	137	EOC	rs17631676	-7.11	2.66×10^{-7}	Critical illness	rs16940665	7.46	1.94×10^{-8}
ABO	Artery Aorta	9	595	EOC	rs495828	5.60	4.92×10^{-3}	Critical illness	rs657152	6.68	5.70×10^{-6}

Infection: reported SARS-CoV-2 infection vs. population; Hospitalization: hospitalized COVID-19 patients vs. population; Critical illness: very severe respiratory confirmed COVID-19 patients vs. population; BC: breast cancer; EOC: overall invasive epithelial ovarian cancer; TWAS: transcriptome-wide association study; GWAS: genome-wide association study; SNP: single nucleotide polymorphism; CHR: Chromosome; ID: identifier; No. SNPs: number of SNPs in the locus; Z: Z value for TWAS.